

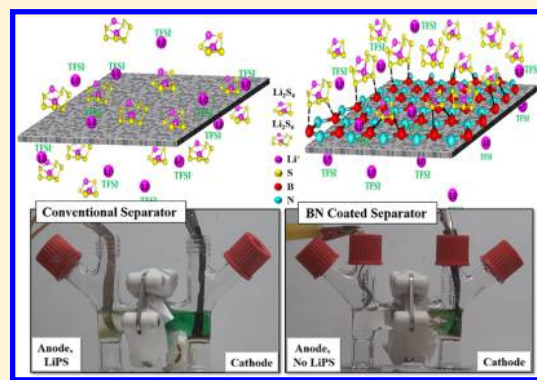
Two-Dimensional Material-Reinforced Separator for Li–Sulfur Battery

Ganguli Babu, Abdulrazzag Sawas, Naresh Kumar Thangavel, and Leela Mohana Reddy Arava*

Department of Mechanical Engineering, Wayne State University, Detroit, Michigan 48202, United States

Supporting Information

ABSTRACT: Li–S batteries are heavily researched as they are capable of meeting the demands of electrification of transport systems, provided their inherent polysulfide shuttling can be prevented to enhance the cycle life. Although several approaches have been made to mitigate the shuttling effect, success is limited due to the poor adsorption capability of polysulfides on the cathode surface. Herein, we propose an efficient approach of using two-dimensional materials with permanent dipoles in the separator to inhibit mass transport of polysulfides from cathode and subsequent parasitic reactions on the metallic lithium anode. Two-compartment H-cell experiments coupled with spectroscopic studies, such as ultraviolet–visible absorption, nuclear magnetic resonance spectroscopy, and Fourier transform infrared spectroscopy, are used to demonstrate the interactions between the two-dimensional materials-modified separator and polysulfide species. Furthermore, electrochemical properties reveal the excellent specific capacity of 1210 mAh g^{−1} and self-discharge studies suggest the feasibility of modified separator for commercial applications.



INTRODUCTION

Li-ion batteries are the forefront power sources in portable electronics and are now the central focus for meeting applications from electric vehicles to space shuttles, to alleviate global warming issues. However, the capability of energy storage is still a major concern due to limited room for developments in conventional lithium-intercalated electrode materials.^{1,2} Beyond the limitations of Li-ion batteries toward efficient energy storage, the lithium–sulfur (Li–S) system shows promise of unraveling the most pressing issues of high energy density and low cost for electric-based transportation.^{2,3} This is mainly attributed to the high theoretical capacity, wide range of operating temperature, low cost, and eco-friendliness of sulfur-based cathodes. However, practical applications of Li–S batteries are still hindered due to short cycle life, poor Coulombic efficiency, poisoning of Li anode, and self-discharge.^{3,4} These performance limitations originate from the insulating nature of sulfur, shuttling effect of dissolved lithium polysulfide (LiPS) species, and their parasitic reactions with the highly reactive negative electrode.^{5–8} Furthermore, dissolved LiPS diffuses into the separator as electrostatic attraction dominates between charged polysulfide species and metallic lithium.^{7,9} Loss of electroactive species then continues with cycling owing to the chemical potential difference, and the concentration gradient leads to mass transport in the electrolyte.

Although remarkable achievements have been realized on the cathode framework by constructing mesoporous carbon–sulfur composites, cycle life and self-discharge on long run are still

major concerns for practical applications.^{10–13} Such deplorable performance is mainly linked to the LiPS shuttling effect, which is inevitable due to poor adsorption of polysulfides on the sulfiphobic carbon surfaces.^{14–17} In this regard, various electrode materials and additives with polarity that interact strongly with dissolved polysulfides have been studied, including polymers,¹⁸ metal oxides,¹⁹ and metal sulfides.^{19,20} Recently, an electrocatalysis approach to enhance the sluggish kinetics of LiPS conversions has gained importance as it is capable of providing both facile charge transfer and adsorption.^{21–26} Nevertheless, electrode structure with the sophistication of pore volume and polarity improves battery performance by minimizing polysulfide shuttling, but the complete prevention is unlikely. On the other hand, introducing “interlayers” between the cathode and separator is an effective strategy to block the PS diffusion toward the anode. Additionally, several materials have been subjected, from simple carbon paper to modified graphene structures with tuning of their conductivity, porosity, and functional groups.^{27–29} However, these structures involve a tedious process to be fabricated as freestanding films, and parasitic reactions with polysulfide species in the separator/interlayer pores due to their conductive nature pose a serious challenge. Moreover, the side reactions of highly active polysulfides and their radical anions with functional groups of carbons and

Received: March 18, 2018

Revised: April 20, 2018

Published: April 30, 2018

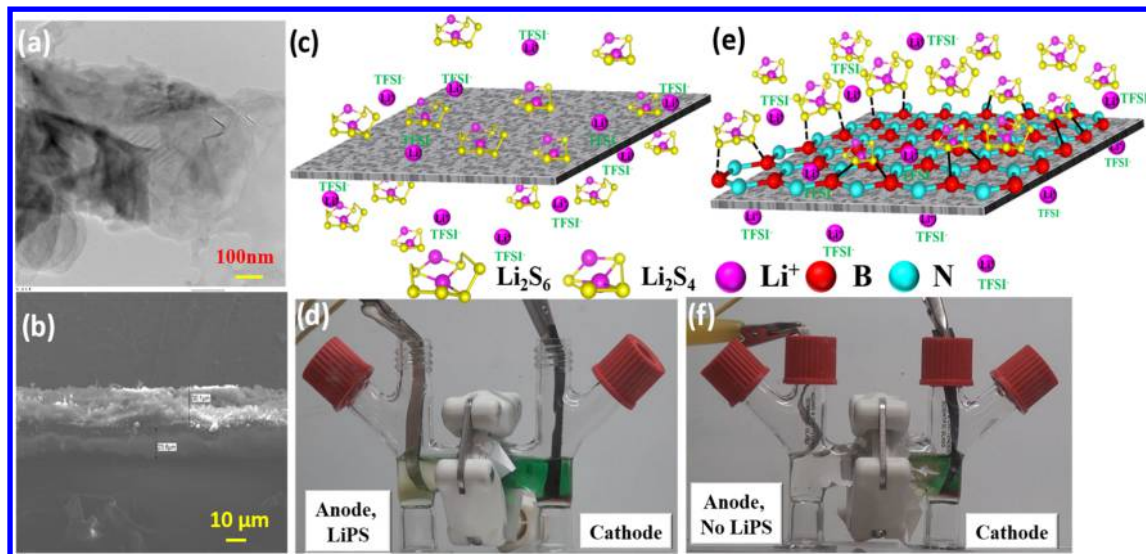


Figure 1. Exfoliation of hexagonal boron nitride and visualization of BN nanosheets-intervened separator for LiPS: (a) TEM image of exfoliated boron nitride nanosheets and (b) cross-sectional SEM image of BN-modified separator. Schematic representations and experimental observation of lithium polysulfides at complete discharged state: (c, d) diffusion through conventional separator and (e, f) stoppage at BN-modified separator via Lewis acid–base interactions.

polymers may lead to performance degradation of the cell. Hence, we hypothesize that the most appropriate solution is to have a multifunctional separator with nonconductive materials and at the same time with strong dipoles to inhibit polysulfide travel toward the anode by adsorbing them strongly.

Herein, separator modification with two-dimensional materials that effectively bind ionic species involved in the system via Lewis acid–base interactions, attracts attention for long-cycling and high-energy-density Li–S batteries. Among various available two-dimensional materials, boron nitride (BN) nanosheets exhibit favorable properties as a separator because it is an insulator, chemically and electrochemically more stable.^{30,31} More importantly, it has a unique character composed of mixed sp^2 -hybridized Lewis acid (boron atoms) and Lewis base (nitrogen atoms), leading to facile bonding with polysulfide species. Boron atoms in BN have high tendency to accept electron pairs from the anion molecules, and a lone pair of electron on nitrogen is capable of attracting the positive end of the polysulfide species (lithium). Together, this leads to an efficient complex formation under an electric field, which mitigates soluble polysulfide diffusion across the separator membrane. Herein, we investigate the interactions between the BN nanosheet-modified separator and polysulfide species in the Li–polysulfide configuration using spectroscopic studies to thereby enhance the electrochemical performance.

■ EXPERIMENTAL METHODS

Fabrication of BN Nanosheets-Modified Separator. To construct a modified separator, boron nitride nanosheets were prepared by a previously reported method with slight modification.³² Here, ultrasonication-assisted liquid-phase exfoliation of hexagonal boron nitride (h-BN, Sigma-Aldrich, 2 μ m) was carried out with a sonic probe instrument. Using sodium cholate hydrate ($C_{24}H_{39}NaO_5 \cdot xH_2O$, Sigma-Aldrich, 99%) as a surfactant material in an aqueous medium with a ratio of 1:5, we sonicated for about 24 h with a time interval of 10 min every 2 h. The homogeneous dispersion obtained was centrifuged at 2000 rpm for about 90 min to segregate the exfoliated BN nanosheets from the residual bulk. Then,

supernatant liquid, which contains BN nanosheets, was drawn off from the solution in a centrifuged tube and used for further experiments. That solution was filtered through a conventional polymer separator (Celgard) and dried for 12 h at 120 °C under vacuum. The amount of uniformly deposited BN nanosheets were calculated per area of the polymer film by adjusting the concentration of BN in solution. Such modified films with different amounts of BN nanosheets were used as a separator in comparison to a bare polymer film.

Preparation of Lithium Polysulfides (Li_2S_4 and Li_2S_8).

In the present study, an active material of sulfur was used in the form of catholyte solutions with the general lithium polysulfides formula of Li_2S_8 or Li_2S_4 in tetraethylene glycol dimethyl ether (TEGDME) solvent. This solution was prepared from stoichiometric amounts of Li_2S and S to form the desired molar ratio of LiPS in TEGDME with effective stirring at 90 °C for 12 h. The catholyte solution (Li_2S_8) used for the electrochemical studies was 10 μ L of 600 mM per cell, which corresponds to 1.52 mg_{sulfur} per cm⁻² of the electrode.

Cell Fabrication. The standard 2032-coin cells were assembled to examine the electrochemical performance of BN nanosheets-modified separator in conventional Li–polysulfides battery configuration. Gas diffusion layer paper was used as the positive electrode with circular cut disks of diameter 12.7 mm. An active material containing catholyte (Li_2S_8) with a molar concentration of 600 mM was used along with an electrolyte composition of 1 M lithium bis(trifluoromethanesulfonyl)imide ($LiTFSI$) and 0.5 M lithium nitrate ($LiNO_3$) in TEGDME.

Materials Characterization. The morphologies of the BN nanosheets and modified separator were characterized by field emission scanning electron microscopy (FE-SEM, JEOL JSM-7600) and transmission electron microscopy (JEOL 2010 TEM, LaB₆ Filament Gun). Chemical interactions between BN nanosheets and dissolved polysulfides were revealed by Fourier transform infrared (FTIR, Varian/Digilab Excalibur 3100) and nuclear magnetic resonance (NMR) spectroscopies (Varian Mercury-400 MHz magnetic field). Electrochemical characterizations were carried out in the potential range of 3.0–1.5 V using ARBIN cycle life tester.

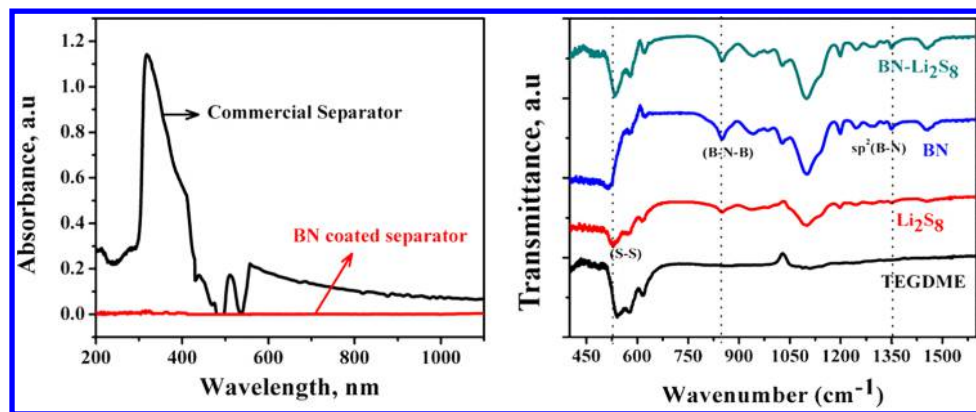


Figure 2. Spectroscopic analysis of lithium polysulfides interactions with BN nanosheets-intervened separator: (a) UV absorption spectra of lithium polysulfides with and without BN modification on separator and (b) FTIR spectra of BN nanosheets and their interactions with lithium polysulfides.

RESULTS AND DISCUSSION

Lithium Polysulfide Interactions with BN Nanosheets-Intervened Separator. Borrowed from the successful exfoliation process for graphene, boron nitride nanosheets were obtained by liquid-phase exfoliation using sonication, which is widely accepted as a feasible method to produce large-scale nanosheets of two-dimensional materials.^{33–35} In a

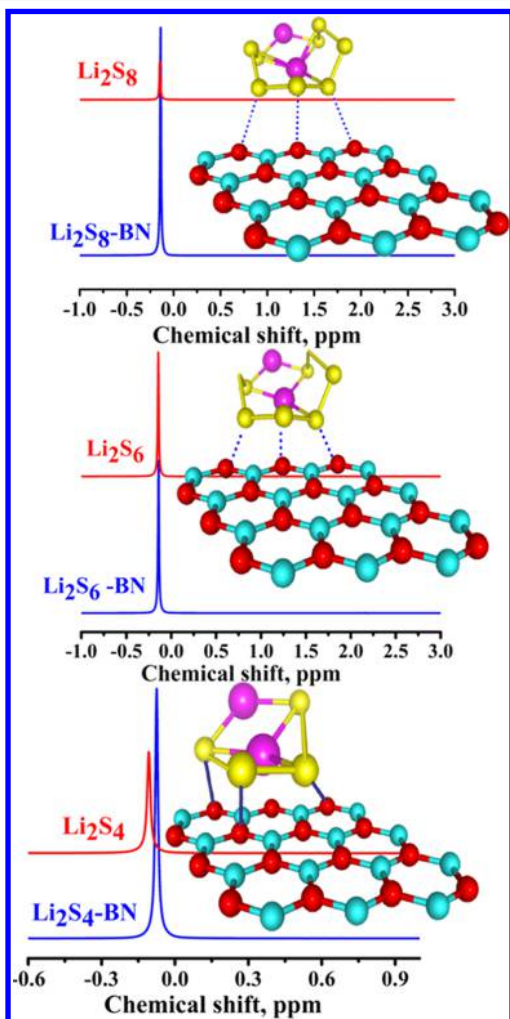


Figure 3. Li⁷ NMR studies of various lithium polysulfide species with and without polar-natured BN nanosheets.

controlled experiment, the energy from the sound waves is effective to overcome the weak forces of attraction between the interlayers of h-BN to produce nanosheets. Using sodium cholate hydrate as the surfactant-disintegrated and stabilized exfoliated nanosheets in a liquid medium, the ratio of BN to surfactant was carefully selected as it predominantly defines the quality of nanosheets. The exfoliated BN nanosheets were collected through repeated centrifugation, which separates out the nanosheets of h-BN from the unexfoliated counterpart. These nanosheets containing solution were washed thoroughly to remove surfactant and vacuum-dried overnight and then subsequently subjected for scanning and transmission electron microscopy (SEM and TEM) studies as shown in the Supporting Information (Figures S1 and S2). Further, TEM images (Figure 1a) revealed a significant disintegration and presence of BN nanosheets, which indicated a successful exfoliation in aqueous solution. The exfoliated nanoflakes were observed to have extensive wrinkling of the edges, as expected from sonication energy generated by sound waves. Like graphene exfoliation by sonication, BN exfoliation resulted in planar objects with small lateral size well below 100 nm, which is suitable to decorate polymer membranes. Hence, modified separator was prepared using a filtration process, wherein Celgard acts as a filter membrane for the solution-BN-contained nanosheets. Prior to use as a separator for the construction of Li–S cells, modified separator was dried under vacuum at 120 °C and were recorded cross-sectional images, as displayed in Figure 1b. The polymer membrane was covered uniformly with a loading of 1 mg cm⁻² and a thickness of 30 μ m.

The interactions of lithium polysulfides and BN nanosheets-modified separator in comparison to pristine separator are schematically shown in Figure 1c,e. A transparent two-compartment H-cell was used to visualize the effect of the BN-modified separator on the stoppage of polysulfides reaching the anode compartment, as shown in Figure 1d,f. The H-cell was constructed using sulfur-impregnated carbon paper, which acts as the working electrode, and metallic lithium, which acts as the counter and reference electrode. During discharge, the liberated Li ions at the anode traveled through the separator to react with sulfur (cathode) to form and simultaneously detach soluble forms of LiPS out of the cathode matrix. In the case of the conventional separator, these intermediate polysulfides tend to pass through to reach the metallic lithium anode, in which parasitic reactions occur and eventually poison the surface for

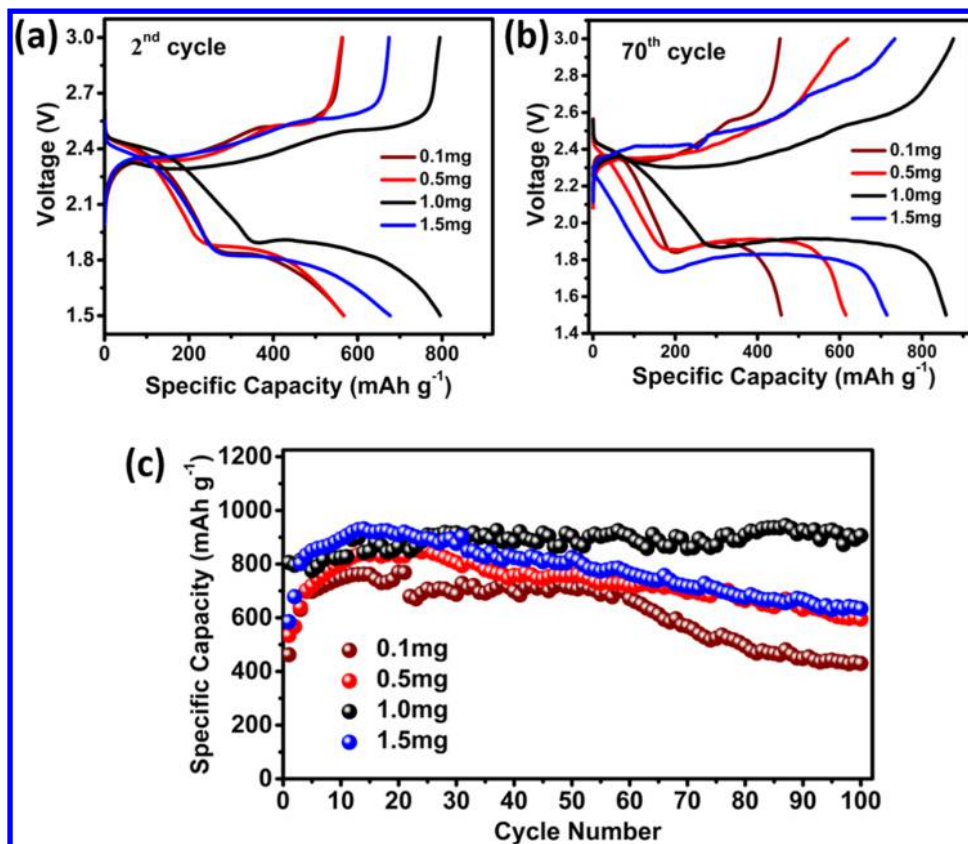


Figure 4. Optimization of BN nanosheets concentration on separator for Li-polysulfide cells. Voltage vs specific capacity profiles at 0.1C rate: (a) 2nd cycle and (b) 70th cycle. (c) Galvanostatic performance of different BN concentrations on separator in Li-polysulfide cells.

subsequent electrochemical reactions (Figure S3, Supporting Information).

Spectroscopic Analysis of Lithium Polysulfides Interactions with BN Nanosheets. The polysulfide species that cross over the separator were detected by UV absorption study as it exhibited a strong absorption peak at 380 nm, shown in Figure 2a. On the other hand, BN nanosheets-modified separator effectively blocked polysulfides by adsorbing them, as evident from the color-free anode compartment, even at deep discharge (Figure 1f). Hence, the lithium anode surface was free from polysulfide poisoning and expected to lead for long cycling with modified separator.

Further, the modified separator at the discharged state was subjected to Fourier transform infrared (FTIR) and Li⁷ nuclear magnetic resonance (NMR) spectroscopy studies to understand the interactions between the BN nanosheets and lithium polysulfide species. In FTIR spectra, LiPS showed its characteristic S–S bending vibration at the fingerprint region at 530 cm⁻¹. Similarly, BN exhibited distinctive peaks at 1349 and 845 cm⁻¹, attributing to the in-plane and out-of-plane bending vibrations of sp²-bonded B–N and B–N–B, respectively. On the other hand, BN–Li₂S₈ samples exhibited a blueshift in polysulfide S–S bending vibrational wavenumbers (538 cm⁻¹) along with BN peaks (Figure 2b). This feature was ascribed to the interaction between the electron-rich LiPS anions and available vacant p-orbital present in boron. The empty orbital in boron made its strong Lewis acid accept the electron pair from the polysulfide species, which acted as a soft Lewis base to donate the electron pair. Such Lewis acid–base interactions substantially prevented the polysulfides to cross

over the separator and thereby have a potential to enhance the stability of the Li–S system.

Moreover, Li⁷ NMR studies revealed the nature of interactions between the lithium of various polysulfides and boron nitride nanosheets of separator (Figure 3). The as-prepared LiPS, viz., Li₂S₈, Li₂S₆, or Li₂S₄, exhibits narrow-line signals of Li⁷ NMR with a very close chemical shift value (ca. -0.14 ppm), indicating that all of the polysulfides had similar nuclei environments, which was consistent with previous reports.³⁶ Conversely, LiPS in conjunction with BN nanosheets showed downfield chemical shift (increased parts per million) and significant increment of line width value. In particular, BN-induced Li₂S₄ showed major changes in NMR parameters among other LiPS. According to an ab initio computational study,³⁷ binding energies are -0.52 eV for Li₂S₄, -0.82 eV for Li₂S₆, and -1.00 eV for Li₂S₈ with respect to a particular material. Similarly, Li₂S₄ may lead to strong adsorption on boron nitride nanosheets and thus reflect in chemical shift in NMR study. As these short-chain polysulfides were responsible for crossing over the separator, trapping such species on BN nanosheets is expected to improve the stability of Li-polysulfides battery. In general, downfield shift was ascribed to the weakness of nucleus electron density with neighboring atoms, and line width denoted the interaction between the surrounding molecules. It is important to note that Lewis acid characteristics of BN effectively accept the electrons from LiPS molecules, which lead to the adsorbing/capturing of soluble polysulfides resulting in a downfield shift. Hence, spectroscopy data clearly revealed that the BN nanosheets effectively captured the dissolved LiPS via Lewis acid–base interactions.

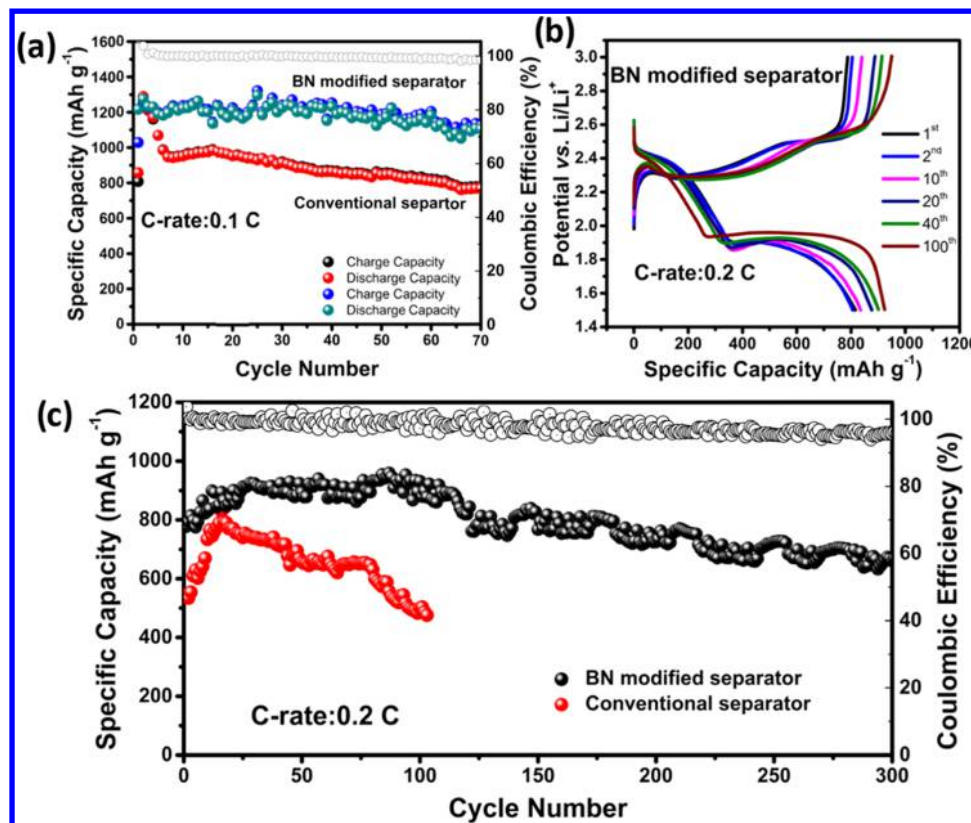


Figure 5. Electrochemical behavior of Li-polysulfide cells with BN-modified separator: (a) cycling behavior of modified separator in Li-polysulfide configuration in comparison to conventional separator at 0.1C rate, (b) charge–discharge profiles of Li-polysulfide battery with BN nanosheets-intervened separator at 0.2C rate, and (c) long-term cycling behavior of lithium polysulfide battery with and without BN-modified separator in the potential range of 3.0–1.5 V at 0.2C rate.

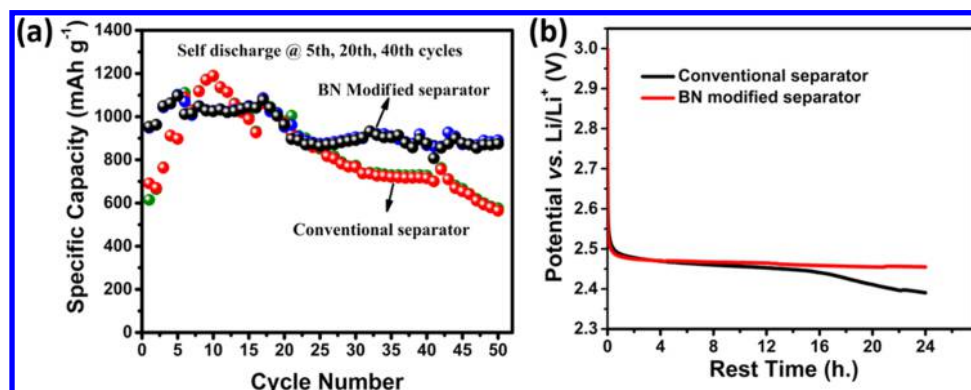


Figure 6. Self-discharge studies of Li-polysulfides battery with BN-modified separator: (a) cyclic performance of BN-modified separator-contained Li-polysulfide cell with intermediate self-discharge for 24 h at 5th, 20th, and 40th cycles and (b) the representative self-discharge profile over 24 h.

Electrochemical Properties. Electrochemical compatibilities of BN nanosheets-modified separator and its unmodified counterpart were evaluated by assembling standard 2032-coin cells. The cells consisted of the gas diffusion layer on carbon paper as working electrode vs metallic lithium foil as counter/reference electrode and Celgard membrane or modified Celgard with BN nanosheets as separator. The electroactive species of sulfur was in the form of LiPS (0.6 M of Li₂S₈) in TEGDME solution containing 1 M lithium bis-(trifluoromethanesulfonyl)imide (LiTFSI) and 0.5 M lithium nitrate (LiNO₃). Electrochemical properties with and without BN nanosheets on separator were measured using 10 μ L of

Li₂S₈ (1.52 mg cm⁻²) at different current rates in a potential window of 3.0–1.5 V.

Prior to testing the modified separator for extended cycling, the quantity of BN nanosheets in a given footprint area (per cm²) of conventional separator was optimized for effective adsorption of LiPS by conducting systematic electrochemical experiments in Li-polysulfides cell configuration. Figure 4 shows the electrochemical performance of Li-polysulfide cells containing modified separator with different concentrations of BN nanosheets. For all of the studied concentrations, typical voltage vs capacity plateaus corresponding to LiPS redox reactions were observed, and their reversibility with cycling was the first indication of separator behavior without short circuit of

the cell (Figure 4a,b). It is important to note that ultralow concentration of BN nanosheets on polymer membrane may not be effective to adsorb all of the dissolution polysulfide species. On the other hand, excess concentration of BN with their insulated nature may result in increased internal resistance of the cell. Therefore, optimized concentration and thickness of BN nanosheets are crucial to obtain desirable features of polysulfides adsorption and hence avoid polysulfides reaching the metallic lithium anode. On careful observation of polarization (the difference between discharge and charge plateau potentials), it was concluded that the BN concentration of 1 mg cm^{-2} was optimum with minimal polarization even after 70 charge–discharge cycles. Such behavior was an indication of the suitability of newly modified separator for long cycling of Li–S battery (Figure 4c). On the basis of stable results, subsequent studies revealed the nature of interactions and extended cycling tests were carried out with 1 mg of BN nanosheets-contained separator.

Figure 5a shows galvanostatic cycling performance of exfoliated BN-modified separator in comparison to a bare separator for 70 cycles at 0.1C rate. This study reveals a specific capacity as high as 1210 mAh g^{-1} with the excellent Coulombic efficiency of $\sim 99.1\%$. Although capacity values are similar for initial cycles, drastic changes were observed as cycling process progresses, for instance, from 10 to 70 cycles, capacity fade was minimal with modified separator, whereas gradual fade was observed with a bare separator. At the end of the 70th cycle, the cell with the modified separator delivered a capacity of 1121 mAh g^{-1} and the cell with the conventional separator displayed a low capacity of 778 mAh g^{-1} due to irreversible mass transport from the cathode. At 0.2C rate, distinct voltage vs capacity plateaus were observed due to well-defined LiPS redox reactions upon a number of cycles (Figure 5b). Such plateaus were attributed to the conversion of long-chain LiPS to medium (Li_2S_x , $6 \leq x \leq 8$) at 2.4 V and subsequent conversion to short-chain LiPS at 2.0 V. Noteworthy to mention that there was stability in polarization even after several cycles, confirming the suitability of newly identified BN nanosheets-modified separator for long cycling of Li-polysulfide battery. Furthermore, owing to large surface area and polarity, exfoliated BN nanosheets were effective in controlling the polysulfide shuttling, enhancing the cycle life as demonstrated in Figure 5c. As expected, Li-polysulfide cell with modified separator exhibited a stable specific capacity of about 810 mAh g^{-1} (Figure 5c) with 83% of capacity retention for 300 cycles. Fluctuation in cell capacity values was observed, which can be originated from the changes in carbon surface area and variations in electrode resistance during cycling. These effects induce the changes in the reactivity of polysulfides with lithium ion, which leads to the variation in sulfur utilization during cycling. In addition, surface area changes lead to irregular plating of discharge ($\text{Li}_2\text{S}/\text{Li}_2\text{S}_2$)–charge (S_8) products in each cycle, thus resulting in variations in the cathode surface resistance and fluctuation in capacity values.

Self-Discharge Studies. Self-discharge deteriorates the battery with age, and cycling and Li–S chemistry are likely to exhibit high self-discharge as their negatively charged intermediate species tend to move away from cathode due to electrostatic attraction forces from metallic lithium.^{38–40} To understand the effect of modified separator, especially with cycling, self-discharge studies were performed in between cycles at 5th, 20th, and 40th cycles, as shown in Figure 6a. It was observed that the capacity drastically faded with intermediate

self-discharges for the conventional separator, whereas stable specific capacity over the cycling was observed with modified separator. Figure 6b evidences the poor self-discharge in bare separator as voltage decays drastically after 12 h. On the other hand, modified separator-contained cell exhibits stability with negligible loss from an open-circuit voltage of 2.49 V; such retention behavior for 24 h was attributed to controlled polysulfide shuttle using polar-natured BN nanosheets.

CONCLUSIONS

In summary, we demonstrated significant improvement in electrochemical performance using BN nanosheets-modified separator. It was anticipated that the high surface area with polar-natured separator induced strong adsorption of polysulfides without crossing over to reach metallic lithium. Visual observations with two-compartment H-cell and spectroscopic studies reveal the interactions between BN nanosheets and polysulfide species under electrochemical cycling. From the detailed electrochemical studies, a high specific capacity of 1210 mAh g^{-1} at 0.1C rate with excellent capacity retention over the number of cycles was realized. More importantly, the rate of self-discharge was almost negligible ($<1\%$) for a fully charged cell with modified separator in 24 h, whereas bare separator-based cell exhibited a high self-discharge of $>4\%$. On the basis of intriguing results, we conclude that ultimate commercialization of Li–S cells lies in stabilizing polysulfide shuttles and protecting metallic lithium from polysulfide poisoning. Hence, designing a compatible and robust separator to achieve stoppage of polysulfides and keeping them intact with cathode matrix could lead to long cycling with minimal self-discharge.

ASSOCIATED CONTENT

Supporting Information

The Supporting Information is available free of charge on the ACS Publications website at DOI: [10.1021/acs.jpcc.8b02633](https://doi.org/10.1021/acs.jpcc.8b02633).

Characterizations of exfoliated BN nanosheets and SEM images of exfoliated boron nitride nanosheets (Figure S1) (PDF)

AUTHOR INFORMATION

Corresponding Author

*E-mail: leela.arava@wayne.edu.

ORCID

Leela Mohana Reddy Arava: [0000-0001-6685-6061](https://orcid.org/0000-0001-6685-6061)

Notes

The authors declare no competing financial interest.

ACKNOWLEDGMENTS

This study was supported in part by the NSF Division of Chemical, Bioengineering, Environmental, and Transport Systems (CBET: 1748363) and ACS Petroleum Research Fund (ACSPRF: 57647-DNI10).

REFERENCES

- (1) Thackeray, M. M.; Wolverton, C.; Isaacs, E. D. Electrical Energy Storage for Transportation—Approaching the Limits of, and Going Beyond, Lithium-Ion Batteries. *Energy Environ. Sci.* **2012**, *5*, 7854–7863.
- (2) Bruce, P. G.; Freunberger, S. A.; Hardwick, L. J.; Tarascon, J. M. Li–O₂ and Li–S Batteries with High Energy Storage. *Nat. Mater.* **2012**, *11*, 19–29.

(3) Yin, Y.-X.; Xin, S.; Guo, Y. G.; Wan, L. J. Lithium–Sulfur Batteries: Electrochemistry, Materials, and Prospects. *Angew. Chem., Int. Ed.* **2013**, *52*, 13186–13200.

(4) Chen, X.; Hou, T. Z.; Li, B.; Yan, C.; Zhu, L.; Guan, C.; Cheng, X.-B.; Peng, H. J.; Huang, J. Q.; Zhang, Q. Towards Stable Lithium–Sulfur Batteries: Mechanistic Insights into Electrolyte Decomposition on Lithium Metal Anode. *Energy Storage Mater.* **2017**, *8*, 194–201.

(5) Liang, X.; Hart, C.; Pang, Q.; Garsuch, A.; Weiss, T.; Nazar, L. F. A Highly Efficient Polysulfide Mediator for Lithium–Sulfur Batteries. *Nat. Commun.* **2015**, *6*, 5682–5689.

(6) Huang, C.; Xiao, J.; Shao, Y.; Zheng, J.; Bennett, W. D.; Lu, D.; Saraf, L. V.; Engelhard, M.; Ji, L.; Zhang, J. Manipulating Surface Reactions in Lithium–Sulphur Batteries Using Hybrid Anode Structures. *Nat. Commun.* **2014**, *5*, 3015–3022.

(7) Hua, W.; Yang, Z.; Nie, H.; Li, Z.; Yang, J.; Guo, Z.; Ruan, C.; Chen, X. A.; Huang, S. Polysulfide-Scission Reagents for the Suppression of the Shuttle Effect in Lithium-Sulfur Batteries. *ACS Nano* **2017**, *11*, 2209–2218.

(8) Xu, N.; Qian, T.; Liu, X.; Liu, J.; Chen, Y.; Yan, C. Greatly Suppressed Shuttle Effect for Improved Lithium Sulfur Battery Performance through Short Chain Intermediates. *Nano Lett.* **2017**, *17*, 538–543.

(9) Rehman, S.; Guo, S.; Hou, Y. Rational Design of Si/SiO₂@Hierarchical Porous Carbon Spheres as Efficient Polysulfide Reservoirs for High-Performance Li–S Battery. *Adv. Mater.* **2016**, *28*, 3167–3172.

(10) Ji, X.; Lee, K. T.; Nazar, L. F. A Highly Ordered Nanostructured Carbon–Sulphur Cathode for Lithium–Sulphur Batteries. *Nat. Mater.* **2009**, *8*, 500–506.

(11) Chen, T.; Cheng, B.; Zhu, G.; Chen, R.; Hu, Y.; Ma, L.; Lv, H.; Wang, Y.; Liang, J.; Tie, Z.; Jin, Z.; Liu, J. Highly Efficient Retention of Polysulfides in “Sea Urchin”-Like Carbon Nanotube/Nanopolyhedra Superstructures as Cathode Material for Ultralong-Life Lithium–Sulfur Batteries. *Nano Lett.* **2017**, *17*, 437–444.

(12) Schuster, J.; He, G.; Mandlmeier, B.; Yim, T.; Lee, K. T.; Bein, T.; Nazar, L. F. Spherical Ordered Mesoporous Carbon Nanoparticles with High Porosity for Lithium–Sulfur Batteries. *Angew. Chem., Int. Ed.* **2012**, *124*, 3651–3655.

(13) Li, G.; Sun, J.; Hou, W.; Jiang, S.; Huang, Y.; Geng, J. Three-Dimensional Porous Carbon Composites Containing High Sulfur Nanoparticle Content for High-Performance Lithium-Sulfur Batteries. *Nat. Commun.* **2016**, *7*, 10601–10610.

(14) Pang, Q.; Nazar, L. F. Long-Life and High-Areal-Capacity Li–S Batteries Enabled by a Light-Weight Polar Host with Intrinsic Polysulfide Adsorption. *ACS Nano* **2016**, *10*, 4111–4118.

(15) Liang, X.; Rangom, Y.; Kwok, C. Y.; Pang, Q.; Nazar, L. F. Interwoven Mxene Nanosheet/Carbon-Nanotube Composites as Li–S Cathode Hosts. *Adv. Mater.* **2017**, *29*, 1603040–1603046.

(16) Li, S.; Mou, T.; Ren, G.; Warzywoda, J.; Wang, B.; Fan, Z. Confining Sulfur Species in Cathodes of Lithium–Sulfur Batteries: Insight into Nonpolar and Polar Matrix Surfaces. *ACS Energy Lett.* **2016**, *1*, 481–489.

(17) Manthiram, A. Materials Challenges and Opportunities of Lithium Ion Batteries. *J. Phys. Chem. Lett.* **2011**, *2*, 176–184.

(18) Chen, M.; Wang, X.; Cai, S.; Ma, Z.; Song, P.; Fisher, A. C. Enhancing the Performance of Lithium–Sulfur Batteries by Anchoring Polar Polymers on the Surface of Sulfur Host Materials. *J. Mater. Chem. A* **2016**, *4*, 16148–16156.

(19) Zhang, Q.; Wang, Y.; Seh, Z. W.; Fu, Z.; Zhang, R.; Cui, Y. Understanding the Anchoring Effect of Two-Dimensional Layered Materials for Lithium–Sulfur Batteries. *Nano Lett.* **2015**, *15*, 3780–3786.

(20) Lei, T.; Chen, W.; Huang, J.; Yan, C.; Sun, H.; Wang, C.; Zhang, W.; Li, Y.; Xiong, J. Multi-Functional Layered WS₂ Nanosheets for Enhancing the Performance of Lithium–Sulfur Batteries. *Adv. Energy Mater.* **2017**, *4*, 1601843–1601850.

(21) Zhou, G.; Tian, H.; Jin, Y.; Tao, X.; Liu, B.; Zhang, R.; Seh, Z. W.; Zhuo, D.; Liu, Y.; Sun, J.; et al. Catalytic Oxidation of Li₂S on the Surface of Metal Sulfides for Li–S Batteries. *Proc. Natl. Acad. Sci. U.S.A.* **2017**, *114*, 840–845.

(22) Li, L.; Chen, L.; Mukherjee, S.; Gao, J.; Sun, H.; Liu, Z.; Ma, X.; Gupta, T.; Singh, C. V.; Ren, W.; et al. Phosphorene as a Polysulfide Immobilizer and Catalyst in High-Performance Lithium–Sulfur Batteries. *Adv. Mater.* **2017**, *29*, 1602734–1602742.

(23) Babu, G.; Masurkar, N.; Al Salem, H.; Arava, L. M. R. Transition Metal Dichalcogenide Atomic Layers for Lithium Polysulfides Electrocatalysis. *J. Am. Chem. Soc.* **2017**, *139*, 171–178.

(24) Al Salem, H.; Chitturi, V. R.; Babu, G.; Santana, J. A.; Gopalakrishnan, D.; Arava, L. M. R. Stabilizing Polysulfide-Shuttle in a Li–S Battery Using Transition Metal Carbide Nanostructures. *RSC Adv.* **2016**, *6*, 110301–110306.

(25) Al Salem, H.; Babu, G.; V. Rao, C.; Arava, L. M. R. Electrocatalytic Polysulfide Traps for Controlling Redox Shuttle Process of Li–S Batteries. *J. Am. Chem. Soc.* **2015**, *137*, 11542–11545.

(26) Babu, G.; Ababtain, K.; Ng, K. S.; Arava, L. M. R. Electrocatalysis of Lithium Polysulfides: Current Collectors as Electrodes in Li/S Battery Configuration. *Sci. Rep.* **2015**, *5*, 8763–8769.

(27) Su, Y.-S.; Manthiram, A. Lithium–Sulphur Batteries with a Microporous Carbon Paper as a Bifunctional Interlayer. *Nat. Commun.* **2012**, *3*, 1166–1171.

(28) Chung, S.-H.; Manthiram, A. A Hierarchical Carbonized Paper with Controllable Thickness as a Modulable Interlayer System for High Performance Li–S Batteries. *Chem. Commun.* **2014**, *50*, 4184–4187.

(29) Ma, G.; Wen, Z.; Jin, J.; Wu, M.; Wu, X.; Zhang, J. Enhanced Cycle Performance of Li–S Battery with a Polypyrrole Functional Interlayer. *J. Power Sources* **2014**, *267*, 542–546.

(30) Luo, W.; Zhou, L.; Fu, K.; Yang, Z.; Wan, J.; Manno, M.; Yao, Y.; Zhu, H.; Yang, B.; Hu, L. A Thermally Conductive Separator for Stable Li Metal Anodes. *Nano Lett.* **2015**, *15*, 6149–6154.

(31) Rodrigues, M.-T. F.; Kalaga, K.; Gullapalli, H.; Babu, G.; Reddy, A. L. M.; Ajayan, P. M. Hexagonal Boron Nitride-Based Electrolyte Composite for Li-Ion Battery Operation from Room Temperature to 150 °C. *Adv. Energy Mater.* **2016**, *6*, 1600218–1600225.

(32) Lin, Y.; Williams, T. V.; Xu, T.-B.; Cao, W.; Elsayed-Ali, H. E.; Connell, J. W. Aqueous Dispersions of Few-Layered and Monolayered Hexagonal Boron Nitride Nanosheets from Sonication-Assisted Hydrolysis: Critical Role of Water. *J. Phys. Chem. C* **2011**, *115*, 2679–2685.

(33) Paton, K. R.; Varrla, E.; Backes, C.; Smith, R. J.; Khan, U.; O'Neill, A.; Boland, C.; Lotya, M.; Istrate, O. M.; King, P.; Higgins, T.; Barwick, S.; May, P.; Puczkarski, P.; Ahmed, I.; Moebius, M.; Pettersson, H.; Long, E.; Coelho, J.; O'Brien, S. E.; McGuire, E. K.; Sanchez, B. M.; Duesberg, G. S.; McEvoy, N.; Pennycook, T. J.; Downing, C.; Crossley, A.; Nicolosi, V.; Coleman, J. N. Scalable Production of Large Quantities of Defect-Free Few-Layer Graphene by Shear Exfoliation in Liquids. *Nat. Mater.* **2014**, *13*, 624–630.

(34) Varrla, E.; Backes, C.; Paton, K. R.; Harvey, A.; Gholamvand, Z.; McCauley, J.; Coleman, J. N. Large-Scale Production of Size-Controlled MoS₂ Nanosheets by Shear Exfoliation. *Chem. Mater.* **2015**, *27*, 1129–1139.

(35) Hanlon, D.; Backes, C.; Doherty, E.; Cucinotta, C. S.; Berner, N. C.; Boland, C.; Lee, K.; Harvey, A.; Lynch, P.; Gholamvand, Z.; et al. Liquid Exfoliation of Solvent-Stabilized Few-Layer Black Phosphorus for Applications Beyond Electronics. *Nat. Commun.* **2015**, *6*, 8563–8574.

(36) Kozen, A. C.; Lin, C.-F.; Pearse, A. J.; Schroeder, M. A.; Han, X.; Hu, L.; Lee, S.-B.; Rubloff, G. W.; Noked, M. Next-Generation Lithium Metal Anode Engineering Via Atomic Layer Deposition. *ACS Nano* **2015**, *9*, 5884–5892.

(37) Li, G.; Wang, X.; Seo, M. H.; Li, M.; Ma, L.; Yuan, Y.; Wu, T.; Yu, A.; Wang, S.; Lu, J.; Chen, Z. Chemisorption of Polysulfides through Redox Reactions with Organic Molecules for Lithium–Sulfur Batteries. *Nat. Commun.* **2018**, *9*, No. 705.

(38) Wang, L.; Liu, J.; Yuan, S.; Wang, Y.; Xia, Y. To Mitigate Self-Discharge of Lithium-Sulfur Batteries by Optimizing Ionic Liquid Electrolytes. *Energy Environ. Sci.* **2016**, *9*, 224–231.

(39) Knap, V.; Stroe, D.-I.; Swierczynski, M.; Teodorescu, R.; Schaltz, E. Investigation of the Self-Discharge Behavior of Lithium-Sulfur Batteries. *J. Electrochem. Soc.* **2016**, *163*, A911–A916.

(40) Ryu, H. S.; Ahn, H. J.; Kim, K. W.; Ahn, J. H.; Cho, K. K.; Nam, T. H. Self-Discharge Characteristics of Lithium/Sulfur Batteries Using Tegdme Liquid Electrolyte. *Electrochim. Acta* **2006**, *52*, 1563–1566.